Ebola Virus VP35 Has Novel NTPase and Helicase-like Activities

Supplementary Data

Ting Shu, Tianyu Gan, Peng Bai, Xiaotong Wang, Qi Qian, Hui Zhou, Qi Cheng, Yang Qiu, Lei Yin, Jin Zhong, Xi Zhou*

Supplementary Figures: 12

Supplementary Tables: 2

Supplementary Figure S1

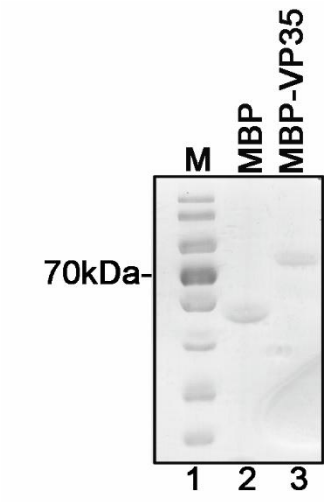

Supplementary Figure S2

A

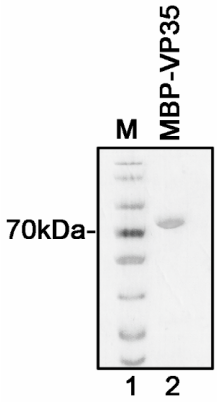

B

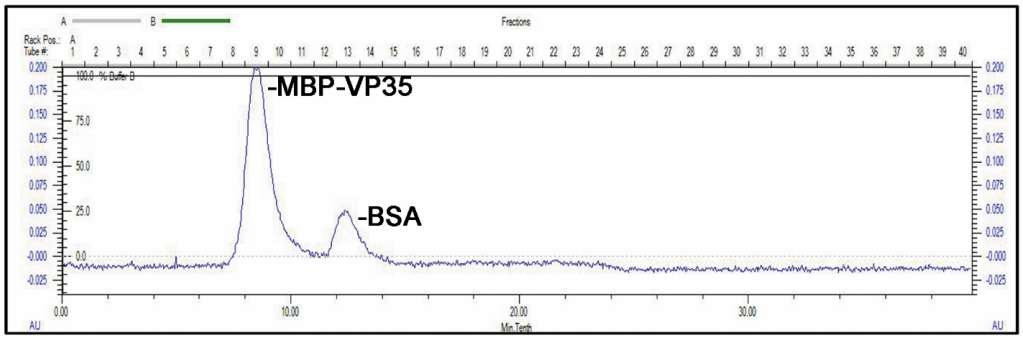

Supplementary Figure S3

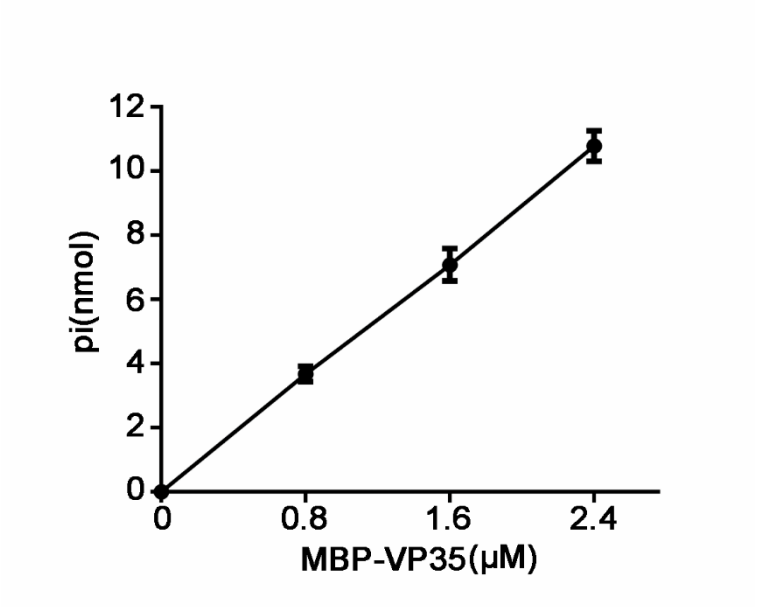

Supplementary Figure S4

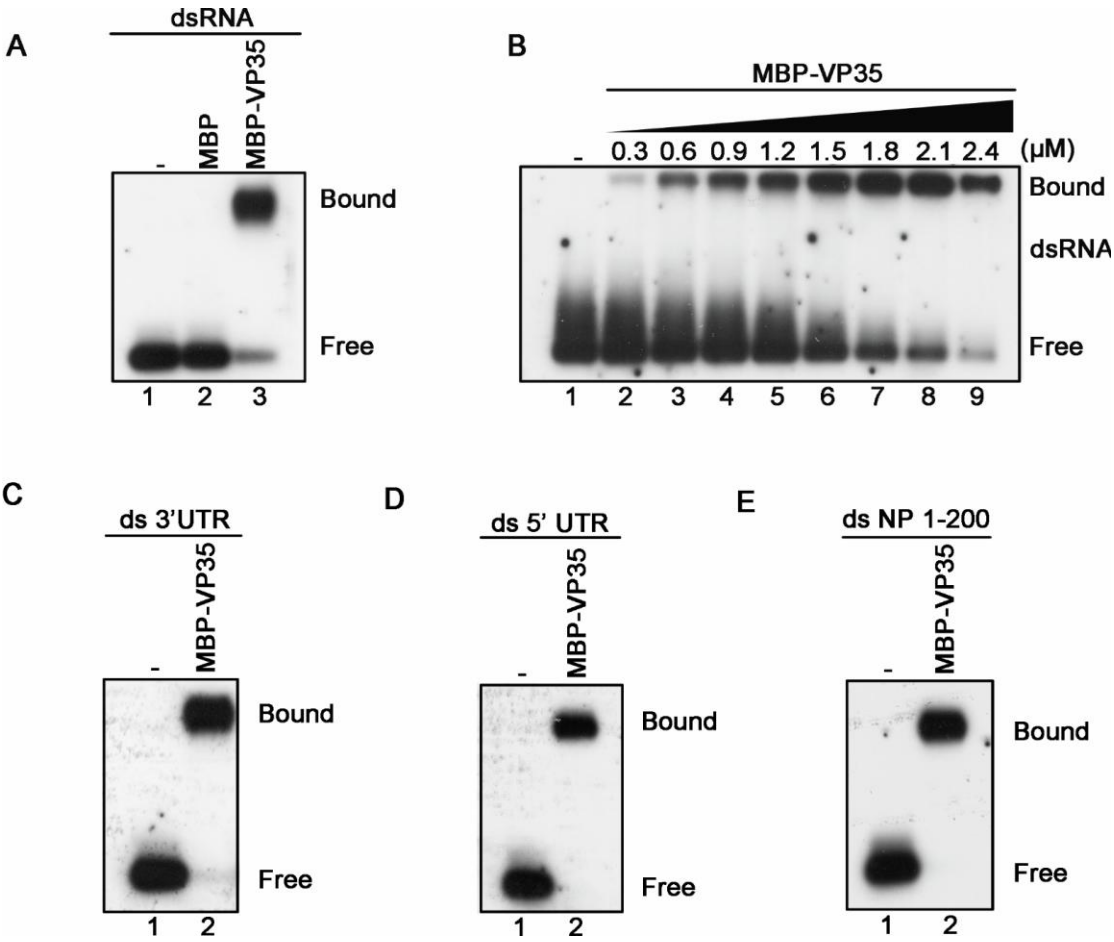

Supplementary Figure S5

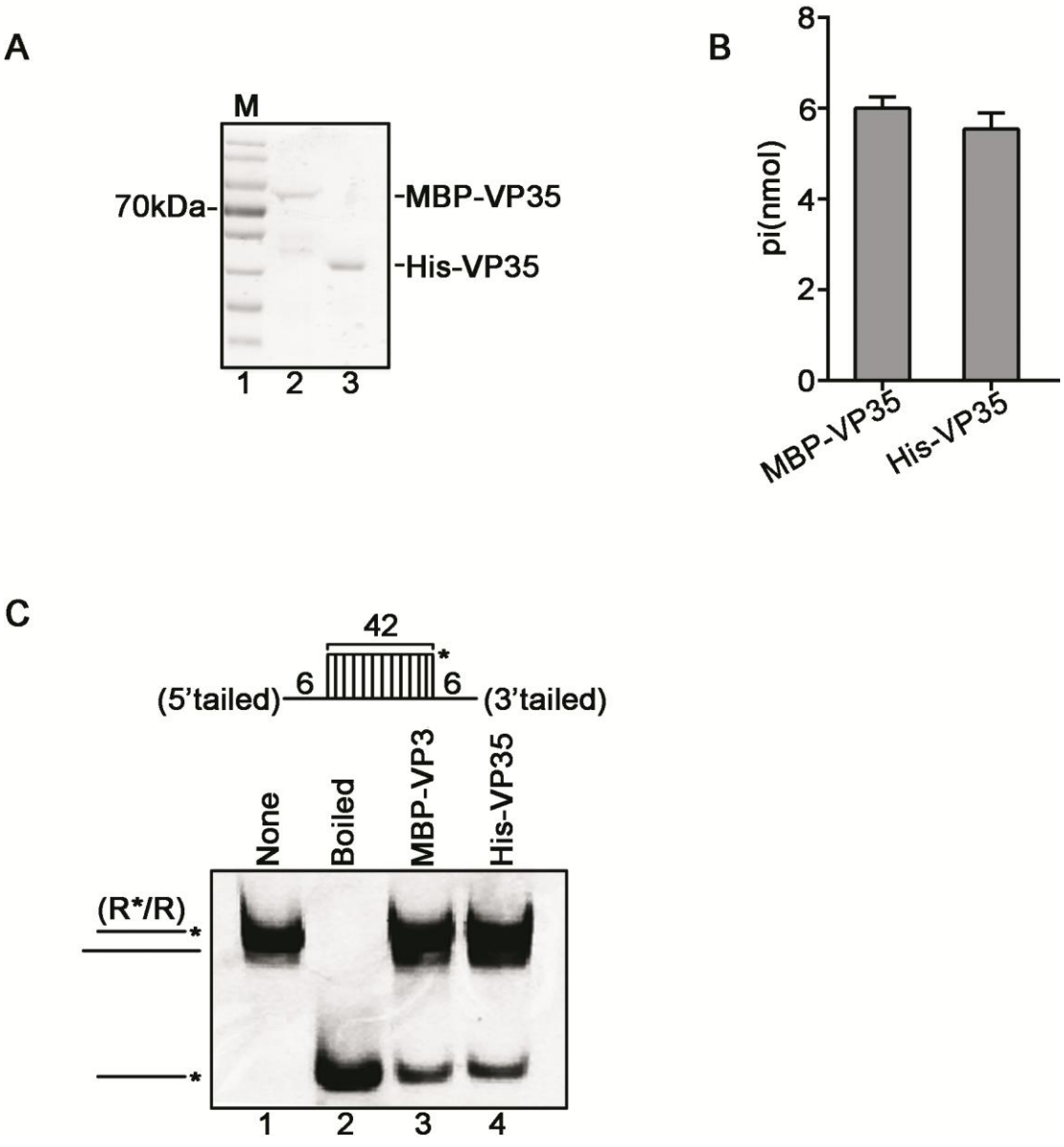

Supplementary Figure S6

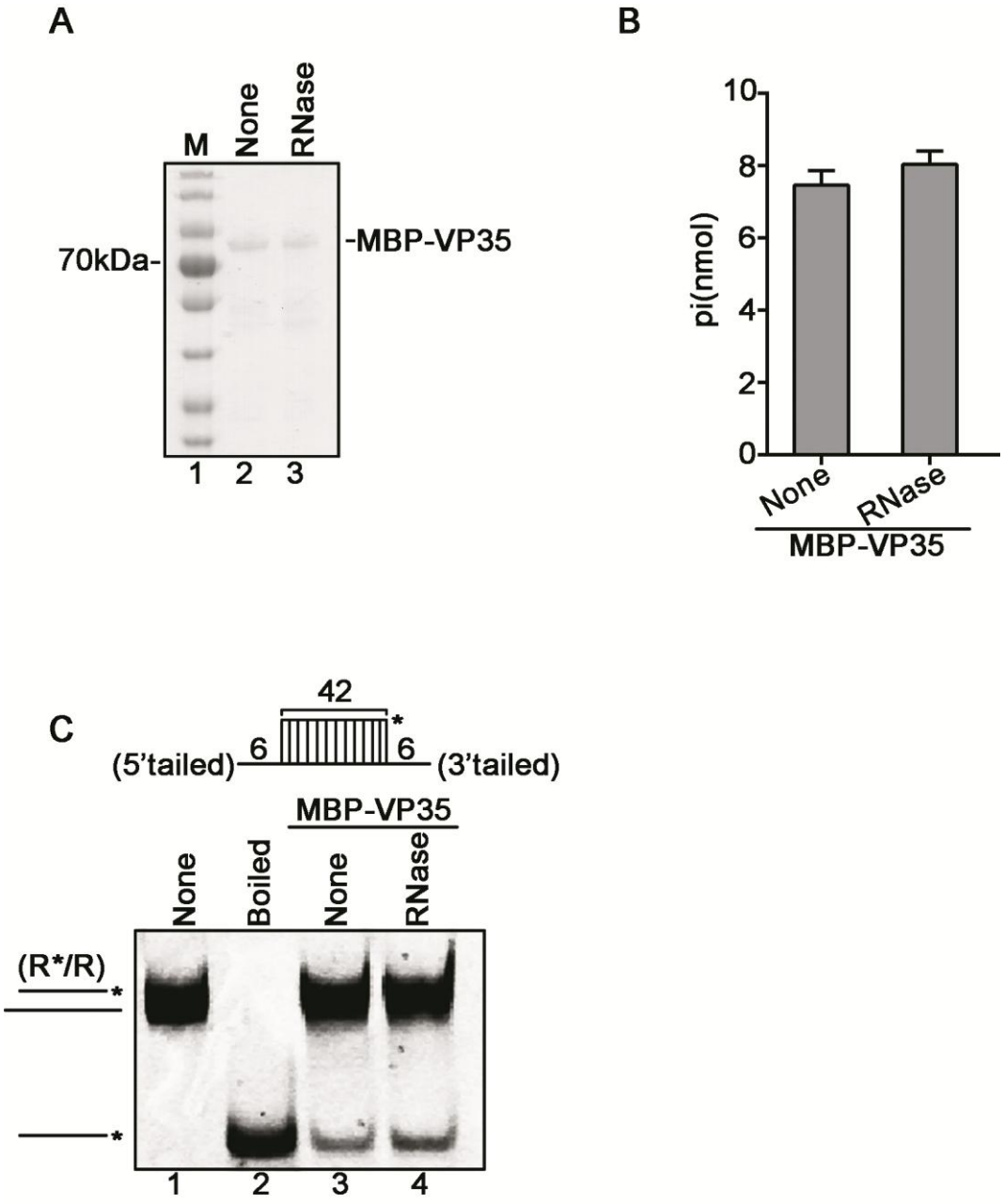

Supplementary Figure S7

A

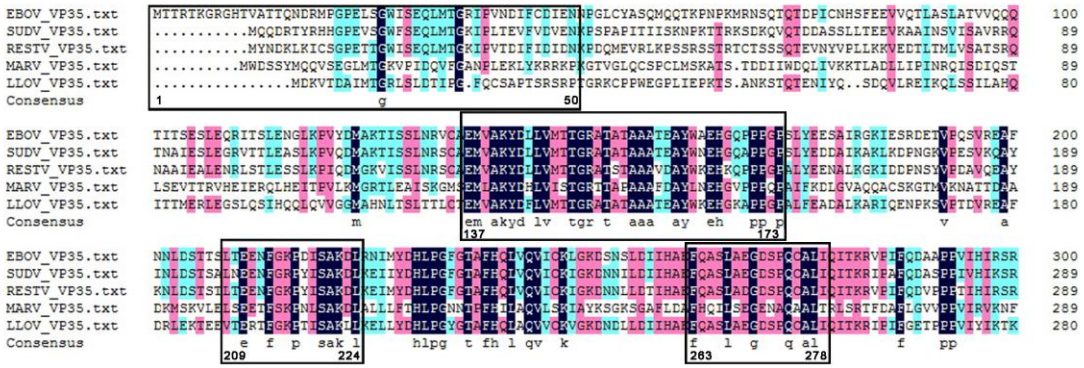

B

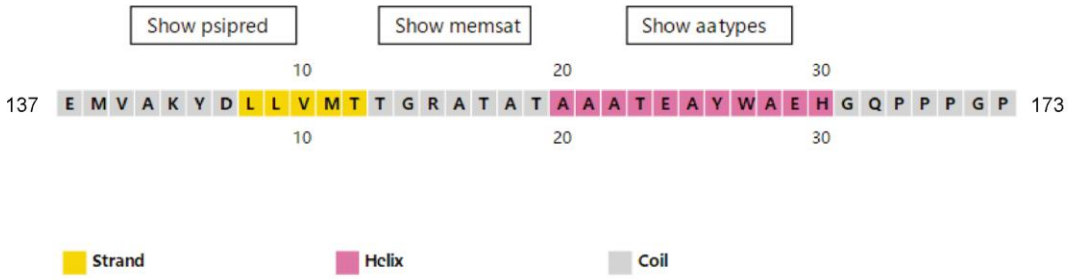

Supplementary Figure S8

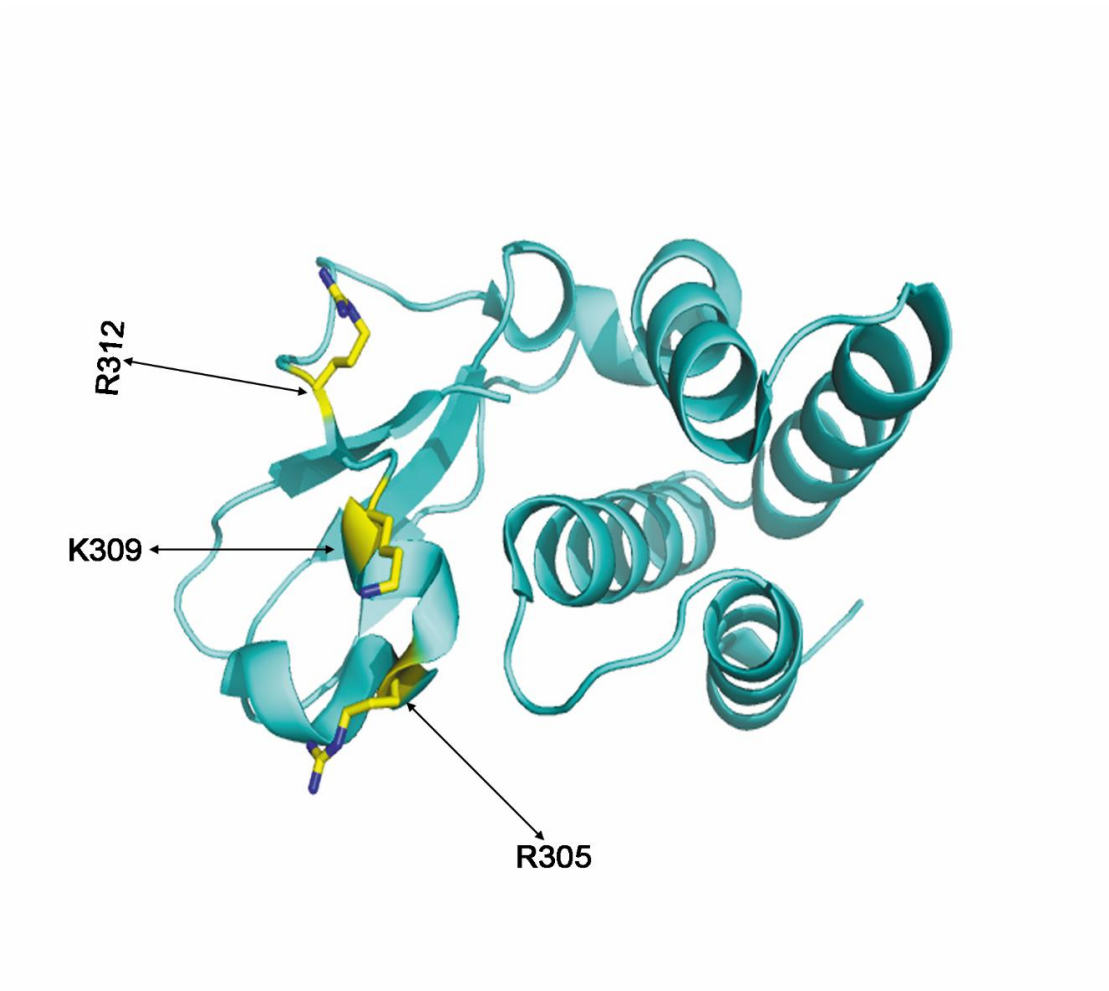

Supplementary Figure S9

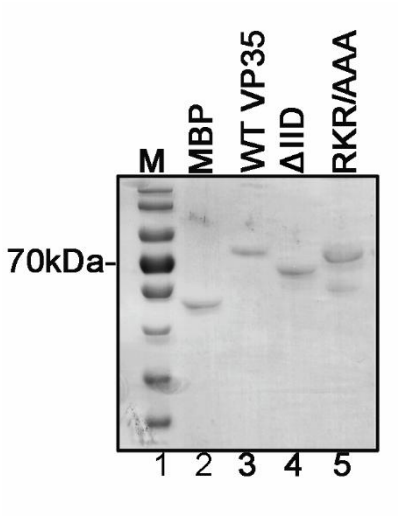

Supplementary Figure S10

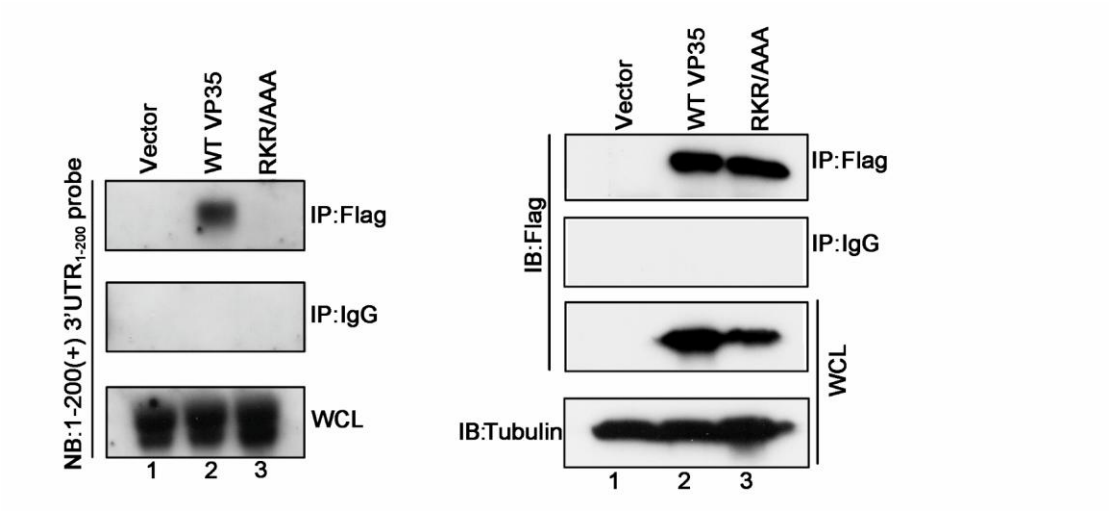

Supplementary Figure S11

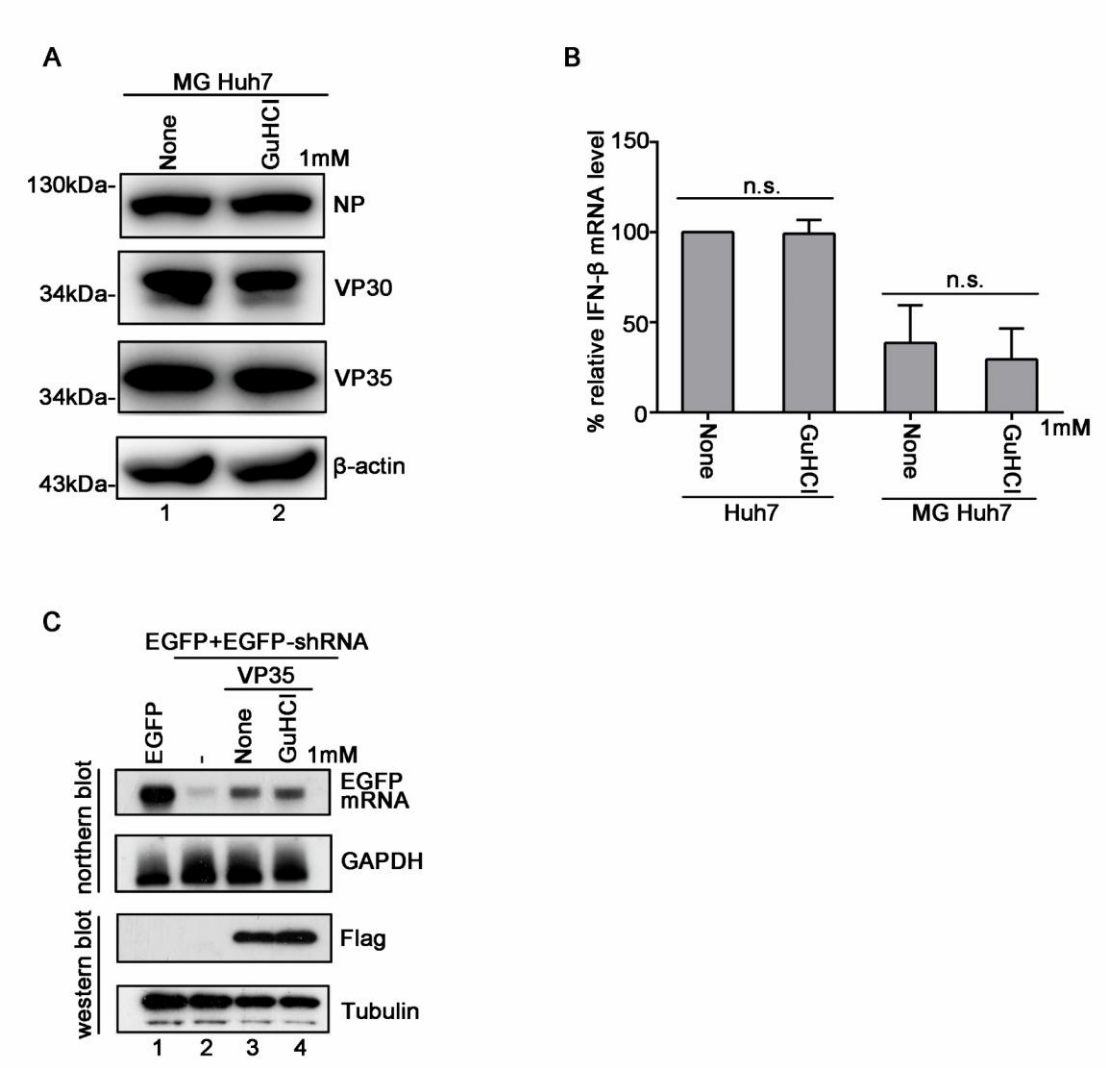

Supplementary Figure S12

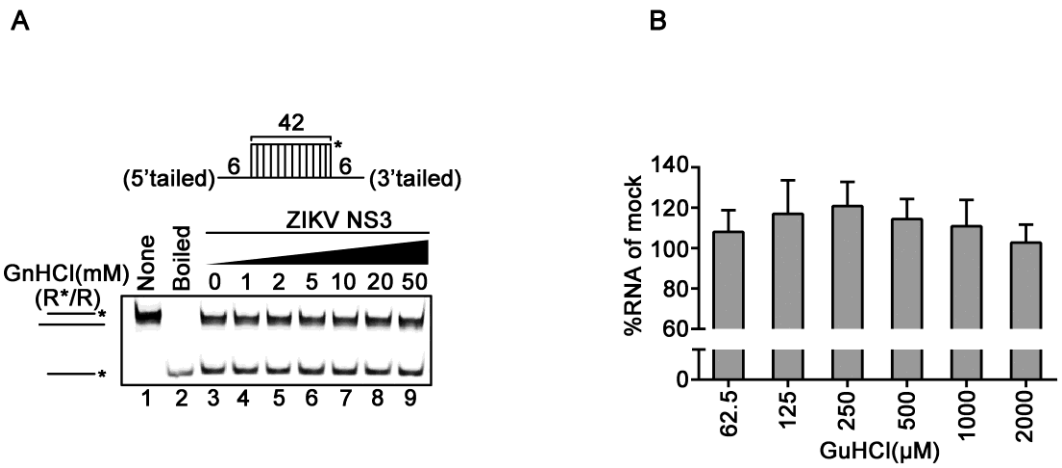

Supplementary Tables

Supplementary Table S1

Primer	Sequence (5`-3`)
VP35-F	CGGAATTCCGATGACAACTAGAACAAAGGGCAGGG
VP35-R	GCGTCGACGCAAATTTTGAGTCCAAGTGTTTTACC
ZIKV NS3-F	CGGAATTCATGAGTGGTGCTCTATGGGATGTGCCTGCT
ZIKV NS3-R	TTGCGGCCGCTTATCTTTTCCCAGCGGCAAACTCCTTG
VP35-△IID-F	GAAAATTTTGGGAAACCTTAATAATAATCGGC
VP35-△IID-R	CCTTTGCCGATTATTATTAAGGTTTCCCAAAATTTTC
VP35-RKR/AAA-F	GGTGACATTCCCGCGGCTTGCCAGGCGAGCTTGGC GCCAGTCCCACCATC
VP35-RKR/AAA-R	GATGGTGGGACTGGCGCCAAGCTCGCCTGGCAAGC CGCGGGAATGTCACC
△1-50-F	CGGAATTCATGCCAGGATTATGCTACGCATCCCAAATGC
△1-50-R	GCGTCGACTCAAATTTTGAGTCCAAGTGTTTTA
△137-173-F	CTCCTCATTGAACAGGGTTTGTGCTTCACTTTATGAAGAAAG
△137-173-R	CTTACCCCGAATCGCACTTTCTTCATAAAGTGAAGCACAAAC
△209-224-F	CAACAATCTAGACAGTACCACTTCAAGAAACATTATGTATG
△209-224-R	CCAGGCAAGTGATCATACATAATGTTTCTTGAAGTGGTAC
△263-278-F	GGACATTATTCATGCTGAGCAAATTACAAAAAGAGTTCC
△263-278-R	GCATCTTGGAAGATTGGAACTCTTTTTGTAATTTGCTCAGCA
Probe-F	TAATACGACTCACTATAGGGTCATAAATTGCTCTCATACAT CATATTGATCTAATCTC
Probe-R	AATTATAAAGAGTGCAGAGTTTATTATGTTGCG

Supplementary Table S2

Oligonucleotide	Sequence (5`-3`) *
RNA1	**CAUUAUCGGAUAGUGGAACCUAGCUUCGACUAUCGGAUAAUC**
RNA2	AAUAAAGAUUAUCCGAUAGUCGAAGCUAGGUUCCACUAUCCGA UAAUGAAAUAA
RNA3	GAUUAUCCGAUAGUCGAAGCUAGGUUCCACUAUCCGA UAAUGAAAUAA
RNA4	AAUAAAGAUUAUCCGAUAGUCGAAGCUAGGUUCCACUAUCCGA UAAUG
DNA1	**CACCACAACCACCACCACCACACCATGG**
DNA2	TGTAGTGCTGCCATGGTGTGGTGGTGGTGGTTGTGGTG GAGCTACGAAC
DNA3	CCGATAGTCGAAGCTAGGTTCCACTATCCG
DNA4	AATAAAGATTATCCGATAGTCGAAGCTAGGTTCCACTATCCGAT AATGAAATAA

*HEX-labeled strands are in boldface.

Supplementary Figure Legends

Supplementary Figure S1. Expression of recombinant EBOV VP35. The purified MBP alone and MBP-fusion VP35 were subjected to 10% SDS-PAGE followed by Coomassie brilliant blue R250 staining. Lane 1, protein marker.

Supplementary Figure S2. Size exclusion chromatography of recombinant EBOV VP35. (A) The MBP-VP35 was purified via MBP column and ion-exchange, and then was examined by 10% SDS-PAGE and Coomassie brilliant blue R250 staining. (B) The purified MBP-VP35 was subjected to the size exclusion chromatography by using a Superdex 200 increase 10/300GL column. Protein elution was followed by UV detection at 280 nm. X axis represents the elution volume (in ml). The major peak comprised most protein (MBP-VP35) that was eluted as a molecular mass of ~600 kDa. The peak of monomeric BSA (~67 kDa) was shown as control.

Supplementary Figure S3. The NTPase activity of MBP-VP35 purified via the ion-exchange and size exclusion chromatography was measured as nanomoles of released inorganic phosphate by using a sensitive colorimetric assay.

Supplementary Figure S4. EBOV VP35 has dsRNA-binding activity. (A) Gel mobility shift assays were performed to evaluate the dsRNA-binding activity of MBP-VP35. MBP-VP35 was incubated with 0.1 pmol DIG-labelled dsRNA substrate, and the complex was analyzed by gel electrophoresis, transferred to membranes and then incubated with anti-DIG antibody conjugated with alkaline phosphatase. Lane 1, no protein supplemented; lane 2, 20 pmol MBP supplemented; lane 3, 20 pmol MBP-VP35 supplemented. Protein-bound and free RNA strands are indicated. (B) Gel mobility shift assays were performed by the indicated increasing concentrations (0-2.4 μM) of MBP-VP35 with 0.1 pmol dsRNA. (C-E) MBP-VP35 were incubated with 0.1 pmol DIG-labelled EBOV 3'-UTR 1-200 nt dsRNA (ds-3'UTR_{1-200}) (C), ds-5'UTR_{1-200} (D), and ds-NP_{1-200} (E), followed by gel electrophoresis. Lane 1, no protein supplemented; lane 2, 20 pmol MBP-VP35 supplemented.

Supplementary Figure S5. The NTPase and RNA helix unwinding activities of His-VP35. (A) His-VP35 purified from baculovirus-expression system was analyzed by 10% SDS-PAGE and Coomassie brilliant blue R250 staining. MBP-VP35 was used as control. (B) His-VP35 (20 pmol) was reacted with 2.5 mM ATP. The NTPase activities of the indicated proteins were measured as nanomoles of released inorganic phosphate by using a sensitive colorimetric assay. (C) The standard RNA helix substrate (0.1 pmol) was reacted with MBP-VP35 or His-VP35 (20 pmol), respectively.

Supplementary Figure S6. The NTPase and RNA helix unwinding activities of RNase A-treated MBP-VP35. (A) MBP-VP35 were treated with or without RNase A, and then analyzed by 10% SDS-PAGE and Coomassie brilliant blue R250 staining. (B) None- or RNase A-treated MBP-VP35 (20 pmol) was reacted with 2.5 mM ATP. The NTPase activities of the indicated proteins were measured as nanomoles of released inorganic phosphate by using a sensitive colorimetric assay. (C) The standard RNA helix substrate (0.1 pmol) was reacted with none- or RNase A-treated MBP-VP35 (20 pmol), respectively.

Supplementary Figure S7. (A) The amino acid sequence alignment of VP35s of EBOV, SUDV, RESTV, MARV, and LLOV. The accession numbers of the VP35 proteins are: AHX24647.1 (EBOV), YP_138521.1 (SUDV), Q91DE0.1 (RESTV), Q6UY68.1 (MARV), and YP_004928136.1 (LLOV). (B) The secondary structure prediction of a.a. 137-173 of EBOV VP35 by using the PSIPRED server. Yellow, β-strand; purple, α-helix; grey, coil or loop.

Supplementary Figure S8. The critical residues for dsRNA binding in the X-ray structure of EBOV VP35 IID. The crystal structure of EBOV VP35 (PDB ID: 3L28) on Protein Data Bank was used for analysis. All presentations of molecular structure graphics were created by using the PyMOL molecular visualization system (The PyMOL Molecular Graphics System). The critical residues for VP35 dsRNA-binding are labeled in yellow.

Supplementary Figure S9. Expression of recombinant EBOV VP35 and its mutants. The WT,

ΔIID and RKR/AAA MBP-VP35 were subjected to 10% SDS-PAGE and Coomassie brilliant blue R250 staining.

Supplementary Figure S10. EBOV VP35 is associated with dsRNA in human 293T cells. HEK293T cells expressing the dsRNA of EBOV 3'-UTR_{1-200} together with the Flag-tagged WT or mutant VP35 (WT and RKR/AAA) were subjected to RNA-IP by using anti-Flag antibody. Northern and Western blots were performed to detect the precipitated proteins and their bound RNAs, respectively. The DIG-labelled positive-stranded RNA of EBOV 3'-UTR_{1-200} was used as probe.

Supplementary Figure S11. GuHCl showed no effect on the viral protein expression and IFN induction in cells expressing EBOV minigenome. (A) Huh7 cells expressing EBOV minigenome (MG Huh7) treated with 1 mM GuHCl were subjected to Western blots by using anti-NP, anti-VP30, anti-VP35 and anti-β-actin antibodies, respectively. The untreated MG Huh7 cells were used as control. (B) Total RNAs were extracted from Huh7 or MG Huh7 cells with or without 1 mM GuHCl treatment, respectively, and the IFN-β mRNA levels were determined by qRT-PCR and then graphed as the percentage of IFN-β mRNA levels from Huh7 cells without any treatment. All data represent means and SD of three independent experiments, n.s., no significance. (C) 293T cells were co-transfected with a plasmid encoding EGFP (0.1 μg) and EGFP-specific shRNA (0.3 μg), together with the plasmid encoding Flag-VP35. At 48 hrs post transfection, Northern and Western blots were performed to detect EGFP mRNA, GAPDH mRNA, Flag-VP35 and α-Tubulin, respectively.

Supplementary Figure S12. The effect of GuHCl on ZIKV NS3 and ZIKV replication. (A) MBP-fusion ZIKV NS3 (20 pmol) was reacted with 0.1 pmol standard RNA helix (as illustrated in the upper panel) in the presence of increasing concentrations of GuHCl. (C) The RNA level of ZIKV was measured at 96 hrs post-treatment of GuHCl with the indicated concentrations (X-axis). Values (Y-axis) were expressed as percentages of those of mock-treated cells. Error bars represent SD values of results from three independent experiments.